Density dependence shapes life-history trade-offs in a food-limited population

Harman Jaggi*[1], Wenyun Zuo[1], Rosemarie Kentie[2,3], Jean-Michel Gaillard[4], Tim Coulson[5], and Shripad Tuljapurkar[1]

[1]Department of Biology, Stanford University, Stanford, CA 94305-5020, USA
[2]NIOZ Netherlands Institute for Sea Research, Den Burg, Texel 1797 SZ The Netherlands
[3]Institute for Biodiversity and Ecosystem Dynamics, University of Amsterdam
[4]Laboratoire de Biométrie et Biologie Evolutive, Université Lyon 1, CNRS, UMR 5558, F-69622 Villeurbanne, France
[5]Department of Biology, University of Oxford, Oxford OX1 2HB, UK

Keywords

trade-offs, life-history, trait covariation, density-dependence, density-dependent selection, LRS

Statement of authorship

HJ performed analyses and writing, WZ, RK, JMG, TC, ST contributed ideas, analyses and writing, RK, TC, contributed data.

Data accessibility statement

The data and code that support the findings of this study are publically available on Zenodo at the link. The zenodo url is https://zenodo.org/records/10839977.

Type of article: Letter

Number of words in the Abstract: 148

Number of words in the main text: 4826

Number of cited references: 61

Number of tables: 1 in the main manuscript and 1 in the Appendix

Number of figures: 5 in the main manuscript and 10 in Appendix

*Corresponding author: harmanjaggi@stanford.edu

Abstract

Quantifying trade-offs within populations is important in life-history theory. However, most studies focusing on life-history trade-offs focus on two traits and assume trade-offs to be static. Our work provides a framework for understanding covariation among multiple traits and how population density influences the traits. Using detailed individual-based data for Soay sheep, we find density strongly shapes life-history trade-offs and distribution of lifetime reproductive success (LRS). At low density, a trade-off between juvenile survival and growth structures life-history variation whereas at equilibrium density (K), trade-off between reproduction and juvenile survival is the major structuring axes. Contrary to Lomnicki's prediction, we find the distribution of LRS is highly constrained at K, with mothers of adult sizes contributing the most to reproduction. Our results offer insights into how high density limits diversity of individual life-histories, advance an understanding of dynamic nature of trade-offs and have implications for evolution via density-dependent selection.

1 Introduction

There is tremendous variation in life-history strategies (Roff 1992; Stearns 1992). The evolution of these strategies is known to be constrained by physiological limitations and in food-limited populations by trade-offs in resource allocation (Stearns 1989; Descamps et al. 2016). Evolutionary theory posits that organisms must allocate limited resources towards different suite of traits to optimize their fitness thereby resulting in trade-offs. Despite evidence for trade-offs, e.g., offspring-size/number (Smith and Fretwell 1974; Venable 1992), immunocompetence and life-history traits in birds (Norris and Evans 2000), trade-offs observed in natural systems are less ubiquitous than those hypothesized by life-history theory (Metcalf 2016). Trade-offs may be difficult to detect because individual variation in resource acquisition is often larger than variation in resource allocation (Van Noordwijk and De Jong 1986), thereby masking life-history constraints in empirical studies. Although life-history theory predicts costs of reproduction and therefore negative correlations among certain traits, individuals can show positive, negative or zero correlations (due to individual heterogeneity or environmental stochasticity) while simultaneously being involved in a classical physiological trade-off (Bell and Koufopanou 1991; Horvitz et al. 1997; Zera and Harshman 2001; Hodgson and Townley 2004; Descamps et al. 2016).

Whether trade-offs within a population are static or change with environmental or demographic conditions is an important question. For instance, as population density varies, individual fitness (i.e. the ability to survive and reproduce) may also vary thereby impacting life-history outcomes. This could result from chance encounters with potential mates or competitive individuals. Thus, variation in population density can generate time-varying selection for different life-history strategies, via density-dependent selection. The concept that selection on life-history traits could vary with population density has been discussed both empirically and in theory by Dobzhansky (1950), MacArthur (1962), and Roughgarden (1971). Pianka (1970) proposed the $r - K$ selection continuum, where r (that refers to intrinsic population growth rate) corresponds to strategies that maximize productivity (i.e. putting all energy into reproduction and producing more offspring) at low density and K (that refers to equilibrium carrying capacity) corresponds to strategies that maximize efficiency (i.e. putting most energy into maintenance and producing only a few fit offspring).

This brings us to our central question:- how do we understand life-history variation at different densities while identifying life-history trade-offs (often masked due to individual variation in resource acquisition)?

Although we often tend to think of trade-offs and density dependence separately, we show here that they are intimately linked. Previous studies (Czesak and Fox 2003; Agrawal et al. 2010) have mostly focused on covariation between two traits but in our research we examine trade-offs among multiple traits by considering the exceptionally detailed long-term observational data collected on Soay sheep (*Ovis aries*) in the St. Kilda archipelago, Scotland. The sheep system is of special interest because this population has been shown to fluctuate dramatically thereby exhibiting potential for density-dependent selection. Coulson et al. (2001) noted population declines of up to 60% occurred when population size was large and winter weather was harsh. This is due to nonlinear interactions between winter weather, population's response to changes in density, and food availability (Grenfell et al. 1992; Clutton-Brock et al. 1996; Coulson et al. 1999). The life-history and physiological mechanisms operating at low density may differ from those operating at high-density (under intense resource limitation), altering the nature and direction of trade-offs.

Our first result is that density dependence shapes life-history trade-offs in a food-limited population of large herbivore. At low densities, we find negative correlations between survival and growth during the juvenile stage (defined in the methods section). However, the intensity and strength of the negative association between juvenile survival and growth is density-dependent and increases with increasing population density. Interestingly, at equilibrium capacity (K), new trade-offs appear and strong negative association between reproduction and juvenile survival structures life-history variation within the population. Multiple trade-offs are revealed by performing a Principal Component Analysis (PCA) on average vital rate functions (survival, recruitment, growth). We find changes in population density affect the relationships among vital rates such as, survival, growth and fecundity. The strength of density-dependent responses of vital rates varies a lot, thereby resulting in trade-offs. Our findings are consistent with life-history theory (Stearns 1992) which predicts trade-offs prevent individuals from being proficient at both surviving and growing to large sizes. In addition, Kentie et al. (2020) found Soay sheep individuals with an optimal life history strategy at high density were different to those having an optimal strategy at low density and thus individuals could not maximise fitness in both high- and low-density environments.

Next, we examined the effects of density on variation in demographic measures. The demographic measures of interest are variation in average vital rate functions, net reproductive rate R_0, and stable age-stage distribution (SSD). We also calculated the distribution of lifetime reproductive success (LRS) using Tuljapurkar et al. (2020) to tease apart trade-offs between allocation in survival and future reproduction. Many empirical studies have consistently revealed that distribution of LRS are often non-normal, zero-inflated and highly skewed (Cabana and Kramer 1991; Tatarenkov et al. 2008). This begs the question: does the distribution of LRS and the skew remain consistent across all population density regimes?

We find the distribution of LRS to be highly constrained at high densities. LRS is an important component of individual fitness and our research predicts density dependence strongly affects the distribution of LRS. In particular, it is the females at prime adult size ($\sim$ 25kg) that contribute the most at high densities, whereas at low densities contributions come from a wider range of body size ($\sim$ 14-25kg). We find a similar pattern for average vital rate functions and stable stage distribution. We base our model and results on previously published Integral Projection Model (IPM) and delifing method presented in Coulson (2012) and Coulson et al. (2006), respectively. Using empirical data and life-history trade-offs between IPM parameters, Kentie et al. (2020) created a covariance matrix that allows us to generate strategies spanning the range of possible individual life-histories that Soay sheep are expected to follow.

The work allows us to examine trade-offs, variation in LRS at low and high densities, and comment on how density can operate. Characterizing trade-offs as a function of population density can not only help elucidate the various determinants of observed life-history variation but will also determine what strategies may be most important for population persistence. Our framework is especially relevant for plant or animal species with individual-based life-history data such as *Hypericum cumulicola* (Quintana-Ascencio and Morales-Hernández 1997), *Heliconia acuminata* (Brooks et al. 2019), *Poecilia reticulata* or commonly Trinidad guppies (Reznick et al. 2006; Bassar et al. 2016), and *Cervus elaphus* or commonly red deer (Gaillard et al. 2003), among others.

2 Model and Methods

We begin with IPM for Soay sheep and then describe sampling life-histories to evaluate trade-offs and the distribution of lifetime reproductive success. IPMs are structured population models that use linear (or linearized) regressions to describe the expected phenotypic trait trajectories (Coulson 2012; Ellner et al. 2016). The IPM consists of four functions that describe how traits such as body size (z) influence survival, reproduction, growth and offspring size. All analysis was carried in R version 4.1.3 (2022-03-10) and the data and code are available here (zenodo link is: `https://zenodo.org/records/10839977`).

For Soay sheep survival, stage transitions and reproduction during a single time interval depend on age and stage (Coulson 2012). Based on Coulson (2012) and Kentie et al. (2020), we model Soay sheep demography in discrete time with population projection matrices (PPMs) structured effectively by stage and add an maximum age of death. That is, we assume that at each age, the stage-structured matrices have same survival and fertility rates until the sheep eventually die off at a certain age. Based on empirical observations, a maximum age of death is set to 16. This enables us to construct a block matrix with stage-structured matrices for each age.

Note that the models are parameterised using female sheep data since the growth rate of Soay sheep population is known to be female-dominant (Coulson et al. 2001) and there is no limiting effect of the number of males for female reproductive output. We use previously published data and IPM for Soay sheep (Coulson 2012; Kentie et al. 2020). The generalized linear functions for survival and reproduction are as follows:

$$S(z,t) = \frac{1}{1+\mathrm{e}^{-(s_0+s_1 z+s_2 N_t)}}$$
$$R(z,t) = \frac{1}{1+\mathrm{e}^{-(r_0+r_1 z+r_2 N_t)}}$$

Here, N_t is the population size at time t. s_0, s_1, s_2 are the intercept, slope and coefficient for body size and density dependence and are our parameters of interest for varying survival. The same holds with r_0, r_1, r_2 and recruitment function. For the parameter values, both survival and reproduction increase with body size z until it eventually saturates.

The growth $G'\left(z' \mid z,t\right)$ and parent-offspring (also called inheritance) $D\left(z' \mid z,t\right)$ functions are described by Gaussian probability density functions. The growth function $G'\left(z' \mid z,t\right)$ is the probability that an individual with body mass z at time t will have a body mass z' at time $t+1$. The parent-offspring function

$D\left(z' \mid z,t\right)$ is the probability that an individual with body mass z at time t will produce an offspring with body mass z' at time $t+1$.

$$G'\left(z' \mid z,t\right) = \frac{1}{\sqrt{2\pi\sigma_g^2[z']}} e^{-\frac{\left(z-E_g[z']\right)^2}{2\sigma_g^2(z')}}$$

$$D\left(z' \mid z,t\right) = \frac{1}{\sqrt{2\pi\sigma_d^2[z']}} e^{-\frac{\left(z-E_d[z']\right)^2}{2\sigma_d^2(z')}}$$

Here, $E_g[z']$ is a linear function that predicts expected body mass and similarly $E_d[z']$ predicts offspring's expected body mass at $t+1$ and are given by $E_g[z'] = \gamma_0 + \gamma_1 z + \gamma_2 N_t$ and $E_d[z'] = \delta_0 + \delta_1 z + \delta_2 N_t$. The function describing variance around the expectation $\sigma_g^2\left(z'\right)$ and $\sigma_d^2\left(z'\right)$ are also linear and are independent of population density. $\sigma_g^2\left(z'\right) = \gamma_3 + \gamma_4 z$ and $\sigma_d^2\left(z'\right) = \delta_3 + \delta_4 z$. The table below summarizes the descriptions of our parameters of interest.

We define Growth Increment as average size in the next time minus size today divided by the size today: Growth Increment, $G = \left(E_g[z'] - z\right)/z = (\gamma_0 + (\gamma_1 - 1)z + \gamma_2 N_t)/z$. The intuition is that individuals reach an asymptotic size based on the stage (say y) at which growth increment (G) becomes 0. We can then partition growth increment until stage y for which individuals reach their asymptotic size. The individuals yet to reach their asymptotic size will have a positive growth increment and is denoted by G. We refer to these individuals as juveniles in this manuscript. This is important to note because we then partition survival based on individuals who have not yet reached their asymptotic size and describe it as juvenile survival (as is described in the next section). Soay sheep are determinate growers, meaning that they grow from conception to some time on their trajectory when they reach an asymptotic size. Effectively, from this time onwards, the sheep should not vary much in size on average during the adult stage and hence we do not consider growth beyond reaching asymptotic size.

We use body mass distributed along 50 size classes as the trait since it is known to affect both survival and reproduction in Soay sheep, and is affected by population density. The IPM functions describe how body size z influences survival, reproduction, growth and offspring size by iterating the distribution of z at $t, n(z,t)$ to $n\left(z', t+1\right)$:

$$n\left(z', t+1\right) = \int \left[D\left(z' \mid z,t\right) R(z,t) + G'\left(z' \mid z,t\right) S(z,t)\right] n(z,t) dz$$

where population size is $N(t) = \int n(z,t)dz$. In matrix terms, the IPM can be written as:

$$\mathbf{n}(t+1) = [\mathbf{D}(t)\mathbf{R}(t) + \mathbf{G}(t)\mathbf{S}(t)]\mathbf{n}(t)$$

Using the IPM functions described above, we construct 50×50 stage-based matrices corresponding the each age for fertility and survival given by $F(z',z) = D(z',z)R(z)$ and $P(z',z) = G'(z',z)S(z)$ (Steiner et al. 2014). We can construct a matrix $\mathbf{P}_a$ which describes probability that an individual in stage z at age t is alive in stage z' at t + 1 which is then used to calculate survivorship denoted by $\mathbf{L}_a$. Similarly, we get $\mathbf{F}_a$ matrix which describes the number of stage z' recruits produced by a female of size z at age a. The net reproductive rate R_0 is calculated as the dominant eigenvalue of the matrix $\sum_a \mathbf{F}_a \mathbf{L}_a$. Note that the summation for ages a is until the maximum age of death (set to 16). In addition, we keep the matrices constant

Table 1: The table provides a list of 16 parameters we use for the four IPM functions (Coulson 2012).

Parameter	Description
s_0	Survival: intercept
s_1	Survival: slope body mass
s_2	Survival: slope population size
r_0	Recruitment intercept
r_1	Recruitment: slope body mass
r_2	Recruitment: slope population density
γ_0	Development, mean: intercept
γ_1	Development, mean: slope body mass
γ_2	Development, mean: slope population size
γ_3	Development, variance: intercept
γ_4	Development, variance: slope body mass
δ_0	Inheritance, mean: intercept
δ_1	Inheritance, mean; slope body mass
δ_2	Inheritance, mean: slope population size
δ_3	Inheritance, variance: intercept
δ_4	Inheritance, variance: slope body mass

for all ages below the age of death which greatly simplifies our analysis. We can do this for different life-histories to understand the pattern of variation within the population. Below we describe how we generate many life-histories based on Coulson et al. (2006) and Kentie et al. (2020).

2.1 Average vital rate functions at SSD to evaluate trade-offs

Coulson et al. (2006) introduced an approach called delifing or leave one out to estimate the contribution of an individual to realized changes in population size and stage-age distribution during a time interval. Using delifing, Kentie et al. (2020) estimated covariance across Soay sheep life-history parameters (such as s_0, s_1, ... and so on) and examined how fluctuating population densities affect within-population variation in life-history strategies. The covariance structure for Soay sheep life history parameters is then used to span the range of possible strategies we expect sheep to follow given the phenotypic life-history trade-offs within and between demographic functions. We sample parameter sets of vital rates from a space of 10,000 life-history strategies (description of delifing in Coulson et al. (2006) and in Methods section of Kentie et al. (2020)).

A parameter set comprises of the 16 parameters: (s_0, s_1, s_2, r_0, r_1, ...), and are described in Table 1. For specific distribution (and values) for each of the parameters we refer to Kentie et al. (2020). We sample 200 such sets from the covariance matrix (using the delifing method). We calculate population growth rate given by λ as the dominant eigenvalue of the age-stage block matrix. The individuals are classified into 50 equal sized stage classes from 1 kg to 38 kg (based on their body size). Thus the dimension of the block matrix is 800×800 because we have 50 size classes and 16 ages. For each parameter set, carrying capacity K is evaluated by finding the population size that results in λ converging to 1. Carrying capacity ratios $(0, 0.5, 1)$ correspond to population size $N = 0$, $N = K/2$ and $N = K$, respectively. The results are robust with respect to the sampling procedure and sample size. Figure A1 in the Appendix shows the range of

equilibrium capacity for the 100 parameter sets.

To explore trade-offs, we calculated vital rate functions such as, juvenile survival (Ss), adult survival (Sb), Recruitment (R), and Growth (G). As discussed before, we partition individuals before they reach asymptotic size based on the stage (say y) at which growth increment becomes 0 and take the average for growth increment until stage y (denoted by G). Similarly, survival for those individuals (Ss) is evaluated by averaging up to the stage (y) and is called juvenile survival. Sheep are considered at their asymptotic size and should not vary much in size on average during the adult stage. Hence we do not consider growth beyond reaching asymptotic size. This way we generate a dataframe/matrix of average vital rates weighted by stable stage distribution (SSD) for 200 parameter sets. Note that the function describing variance around the expectation $\sigma_g^2\left(z'\right)$ is independent of population density so we don't consider it (we verified using calculations and the variance is small).

To understand trade-offs, we perform a PCA on average vital rate functions discussed above and the correlation plot at three densities. We evaluate the carrying capacity K for each parameter set described above and then calculate the average vital rate functions at the carrying capacity. This gives us a dataframe with 200 values for the 4 vital rate functions of interest (Ss, Sb, R, G). We can then repeat the exercise by calculating the average vital rate function at any ratio of carrying capacity. We predict the effects of density by focusing on population $N = 0,\ N = K/2,\ N = K$. We also explore the results from increasing the equilibrium capacity beyond $N = K$.

Since we are interested in examining the influence of population density on vital rate covariations, we note the derivative of $S(z,t)$ and $R(z,t)$ with respect to N is of the form:

$$\frac{\partial S(z,t)}{\partial N} = s_2 S(z,t)(1 - S(z,t))$$
$$\frac{\partial R(z,t)}{\partial N} = r_2 R(z,t)(1 - R(z,t))$$

Since $S(z,t)$ and $R(z,t)$ are both logistic functions, they are always between 0 and 1. The values of s_2 and r_2 are negative and thus the derivative of $S(z,t)$ and $R(z,t)$ with respect to N will always be negative. We plot $S(z,t)$ and $R(z,t)$ for different values of N in the Appendix (Figure A2).

2.2 Lifetime Reproductive Success (LRS)

LRS measures the number of offspring an individual produces over its lifespan and individuals may produce 0, 1, 2... offspring, until they eventually die. The number of offspring produced during a time interval depends on the age and stage at the beginning of the time interval and is specified by probability distributions of producing $0, 1, 2, \cdots$ offspring. The distribution is assumed to be Bernoulli since Soay sheep produce either 0 or 1 offspring in a time interval and we ignore twinning (less than 1.9% of the offspring recruited are twins Simmonds and Coulson (2015)). Thus, following Tuljapurkar et al. (2020), we can compute the exact distribution of LRS for the age-stage-structured vital rates.

Tuljapurkar et al. (2020, 2021) developed an exact analysis to calculate the probability distribution of LRS for species described by age + stage models. The method assumes the empirical vital rates are known for a large cohort of individuals, for each st(age) of individuals life cycle. We use the method detailed in (Tul-

japurkar et al. 2020) to compute LRS distribution of Soay sheep individuals and examine demographic heterogeneities in the distribution.

The mean of LRS distribution is the net reproductive rate R_0. We decompose R_0 into probability of having no offspring and R_0 conditional on making non-zero offspring, denoted by γ and is easily calculated as one minus the probability of reproductive failure (β_0).

$$R_0 = \sum_{k \geq 0} k\beta_k = \sum_{k>0} k\beta_k$$

$$\beta_0 = 1 - \sum_{k>0} \beta_k$$

where β_k is the probability of having k offspring. We are interested in $\gamma = \sum_{k>0} \beta_k$, which is the mean LRS conditional on reproducing at least once.

3 Results

3.1 Trade-offs and Correlations at different densities

Using PCA, we examine trade-offs between average vital rate functions evaluated at SSD, juvenile survival (Ss), adult survival (Sb), recruitment (R), and growth increment for individuals before they reach asymptotic size (G) (Figure 1).

Most (between 68 and 80%) of the observed variation in vital rates is explained by the first two principal components. The variance along the first principal component is explained by the trade-off between survival and growth until individuals reach their asymptotic size at low densities. However, at high densities the trade-off between survival and reproduction becomes most significant and structures life-history covariation as shown in Figure 1 and Table A3 (sign for Reproduction and juvenile survival are opposite). We validated our results using broken stick model and identified principal components whose eigenvalues surpass those predicted by the broken stick model (Figure A5 in Appendix). The variation captured by these components reflects significant underlying patterns in our data and is not a result of chance alone.

We find negative correlation between Growth Increment (G) and Survival (Ss) for individuals before they reach asymptotic size is present at all densities and corresponds to the main structuring axis of life history variation across individuals. As we increase the density to equilibrium capacity (K), the strength of the negative correlation between growth increment and survival further increases (Figure A6 in Appendix). Interestingly, the trade-off between reproduction and juvenile survival is the largest at high population densities and reveals itself only in the density dependent case in the bottom panel of the figure A4. In addition, juvenile survival negatively correlates with all other vital rates- recruitment (R), adult survival (Sb) and growth (G).

The figure A4 in Appendix shows the intensity of the association between juvenile survival, growth and reproduction at the three densities. This association has an increasing importance in shaping life history variation with increasing density and that at high densities there is a three-way trade-off between survival,

growth increment, and recruitment.

What happens beyond equilibrium carrying capacity? We examine the demographic consequences when the population density increases beyond the equilibrium carrying capacity (Figure A7 in the Appendix). We find that now the trade-off between survival and reproduction weakens as population density is increased beyond carrying capacity (K) but the growth-survival trade-off remains strong as shown in the correlation and PCA plot evaluated at population density $N = (1.2)K$ and $N = (1.4)K$.

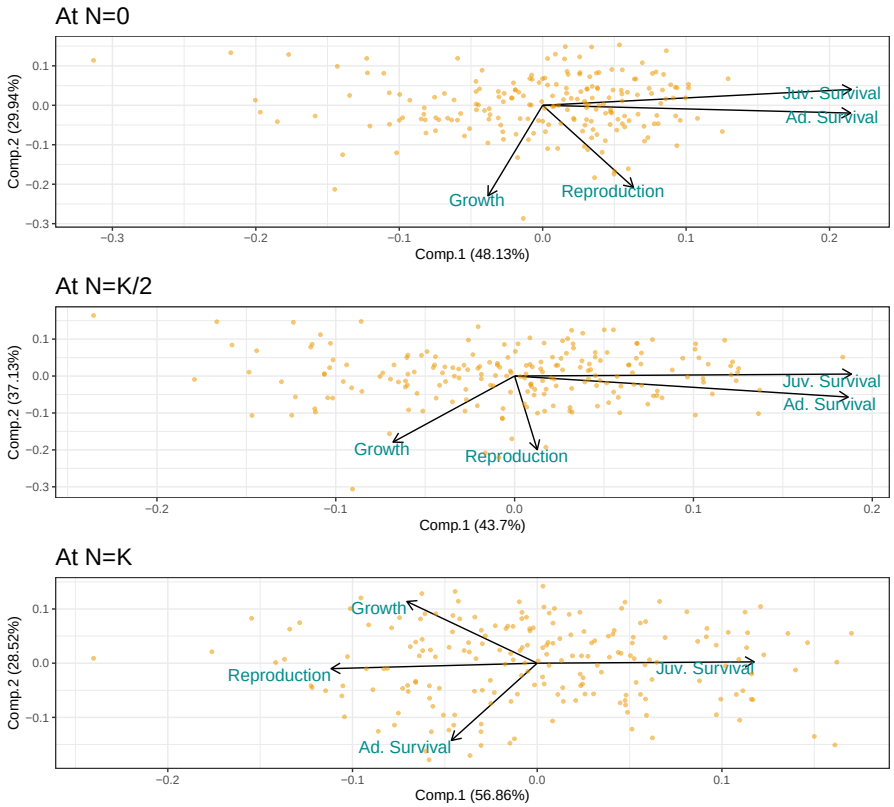

Figure 1: PCA results for average vital rate functions at SSD. Each panel corresponds to a density scenario. Top most panel is for $N = 0$ case, followed by $N = K/2$, and $N = K$. Here Ss and Sb correspond to average survival (over 200 life-histories) for individuals before and after they reach their asymptotic size, respectively. Similarly, GIs and GIb is the average growth increment from one time to next for individuals before and after they reach their asymptotic size, and R is the average reproductive output.

3.2 Variation in R_0 at different densities

Having identified the dynamic nature of trade-offs with population density, we wanted to examine density effects on demographic measures such as the net reproductive rate (R_0) (same as mean of LRS) and the stable stage distribution. The R_0 is calculated as the mean of the LRS distribution as well as through the age-stage block matrix (results are consistent). As discussed in the methods section, the model is age and stage-based in the sense that at age 16 we set survival to 0.

Figure 2 depicts the decrease in variation in R_0 as a function of population size and we find both mean and variance of R_0 decreases with increasing N. Since both $S(z,t)$ and $R(z,t)$ are monotonically decreasing

in N, R_0 is also a monotonically decreasing function of N. The key point here is the extent of variation in R_0 for a density-independent ($N = 0$) and density-dependent case. The life-histories with large R_0 at low densities are highly impacted.

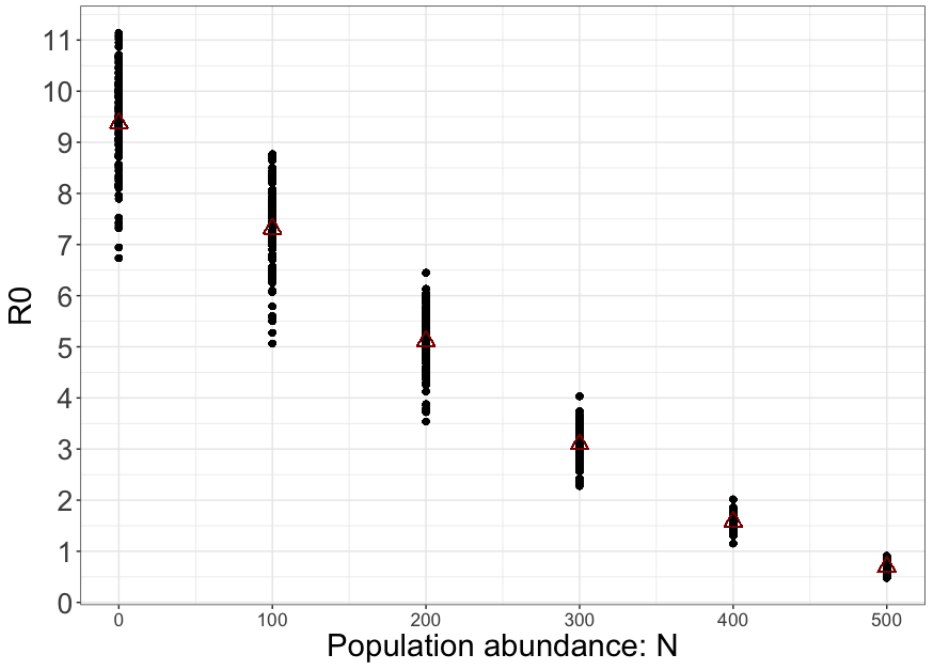

Figure 2: R_0 as a function of population size. Each black point represents the R_0 for a life-history evaluated at the particular population size. The red triangle denotes the mean of the 200 life-histories from the covariance matrix.

What factors contribute to decline in R_0? We explore the question by understanding the variation in SSD and mother's size distribution at three population sizes ($N = 0$, $N = K/2$ and $N = K$). Since we are interested in sizes (stages), we examine the SSD for stage-based matrix population model. For each sample of parameter set, we estimate the equilibrium size K and calculate the stable stage (size) distribution (Figure A8 in Appendix). We take the average of SSD over 200 of our samples. Then we repeat by setting the population size at 0 and at $K/2$.

As population size increases from 0 to equilibrium population size K, the distribution/proportion of adults increases while the proportion of juveniles decreases, in contrast with density-independent case which has a higher proportion of juveniles (as shown in Figure A8 in the Appendix). We observe the same when we examine the distribution for mother's size (scaled by SSD) as shown in Figure 3. We find the range of mother's size to be less at higher densities thus contributing to lower R_0. Thus, as density increases there is a concentration toward individuals of large prime sizes (about 25kg) and contribution from individuals of sizes between 15-25kg is diminished. This is interesting because not only is there more competition and resource scarcity at high density but there are also less individuals contributing to reproduction. Thus, the focus is to produce few extremely fit offspring and this aligns with r-K selection theory.

Lastly, we examine the relationship between R_0 at density-independence (by setting $N = 0$ to evaluate the matrices) and the equilibrium size K for the parameter sets. Figure A9 (in the Appendix) shows K and R_0 are slightly negatively correlated as found in Kentie et al. (2020). Our results align with Pande et al. (2020,

2022) as they show mean population growth rate when rare (a measure of invasibility Chesson (2003)) is limited in its use as a metric for persistence.

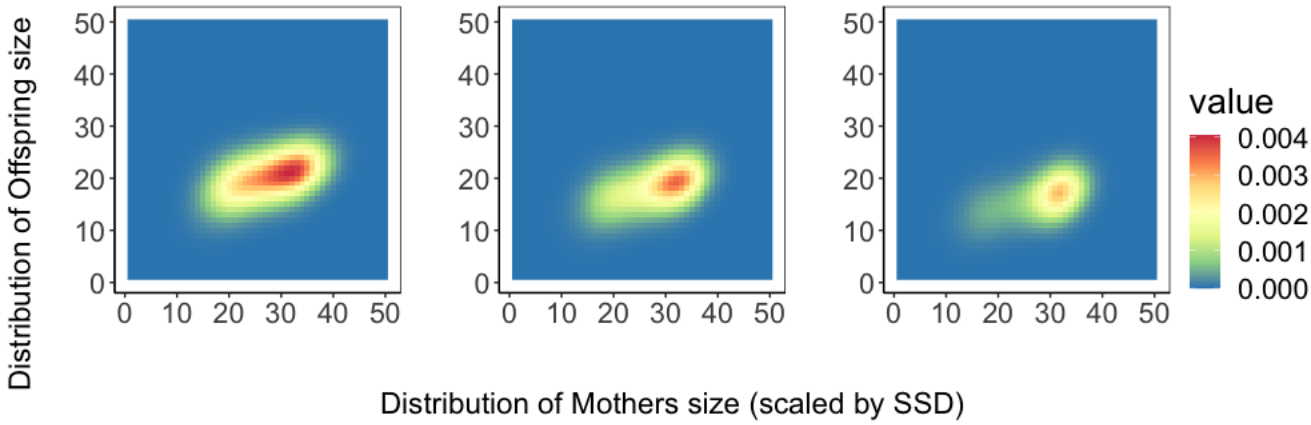

Figure 3: Plot for the distribution of Mothers size: on the x-axis we have mother's size distribution scaled by SSD and on the y=axis we have offspring size. Each panel corresponds to a density scenario. Left most panel is for $N = 0$ case, followed by $N = K/2$, and $N = K$.

3.3 Variation in vital rates

This section examines the relationship between average vital rate functions at SSD and mean lifetime reproductive success conditional on making at least one offspring (given by γ). We evaluate average juvenile survival (weighted by SSD) for our parameter set and regress against γ evaluated at the three population sizes (Figure 4).

We find although increase in juvenile survival increases γ_0 at low densities, near equilibrium size, R_0 and γ_0 are indifferent to changes in juvenile survival. We repeat the above by considering the relationship between average recruitment and average growth (at SSD) with γ_0 and the results are similar to that for juvenile survival. Figure 4 show the constraints operating at high densities and equilibrium population sizes and perhaps how the mechanisms operating at different population sizes are different.

3.4 Variation in LRS trajectories at different densities

We calculate the distribution of LRS (Tuljapurkar et al. 2020) for the 200 life-histories sampled from the covariance matrix. From Lomnicki (1978)'s work, we hypothesize a higher variation in LRS among females at high than at low density and our results are different from Lomnicki's prediction (Figure A10 in Appendix). The LRS trajectories show considerable variation at $N = 0$ which is not reflected at high densities since the size distribution is skewed toward individuals of large body sizes. It is remarkable how the

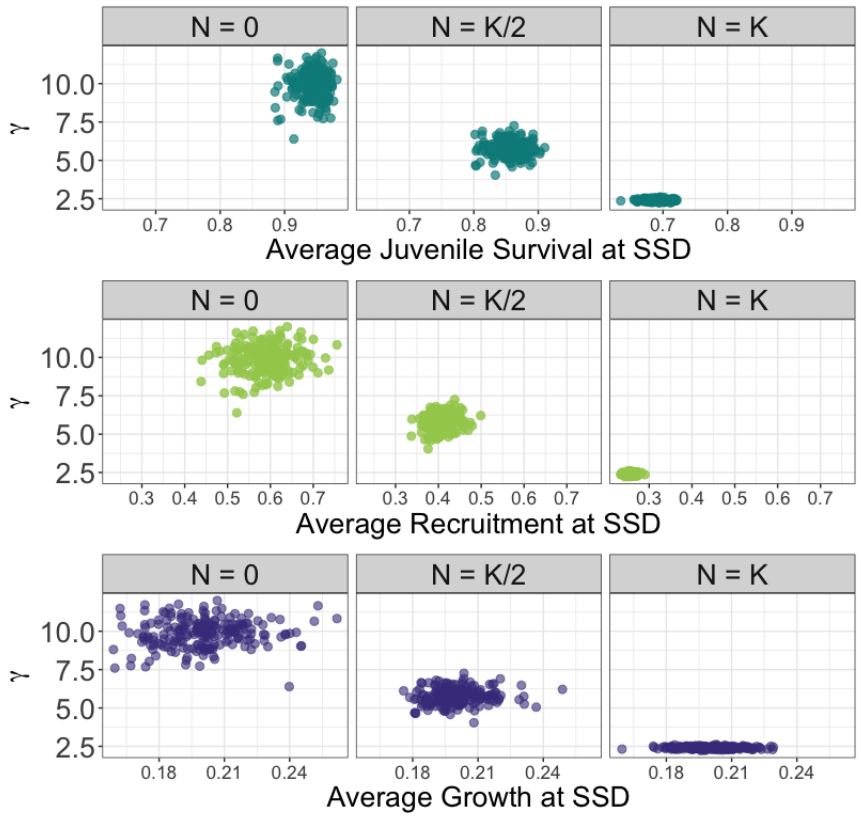

Figure 4: Trends for average vital rates at different population densities. On the y-axis is γ, that is the mean lifetime reproductive success conditional on making at least one offspring. The first three panels (left to right at $N = 0$, $N = K/2$, and $N = K$) have average juvenile survival rates at SSD on the x-axis, the second panel has average recruitment at SSD, and the last three panels have average growth at SSD.

shape of the LRS distribution varies for the three density scenarios. At $N = K$ (right-most panel in Figure 5), the probability of havin zero offspring is higher when compared to the case when $N = 0$. For animals (as discussed in the Methods section), the probability of having zero offspring corresponds to juvenile mortality. The results are consistent with empirical observations since field studies find high juvenile mortality at equilibrium population sizes than at low densities.

To further examine trade-offs from LRS distributions, we generated life-histories where survival parameters (s_0, s_1, s_2) are sampled from the covariance matrix and the rest of the 13 parameters are fixed to their mean values. Similarly, we fixed all parameters to their mean values but recruitment parameters (r_0, r_1, r_2). The top panel of Figure 5 shows the average distribution of lifetime reproductive success and the confidence intervals for each offspring number. In the bottom panel of 5, we find at low population density and despite fixed survival, small variation in fertility by chance alone can lead to higher or lower probability of having zero offspring. In the Appendix (Figure A10), we also calculate the distribution when all parameters are perturbed and our results remain consistent.

Finally, we fixed all parameters but growth parameters. Our expectation was the additive effect of survival (only) and growth (only) would be greater than the effect of varying both survival and growth parameters together. We find slight evidence for such a trade-off for low offspring (0, 1 and 2) but further analysis is needed to uncover the trade-off (Figure A11 in Appendix).

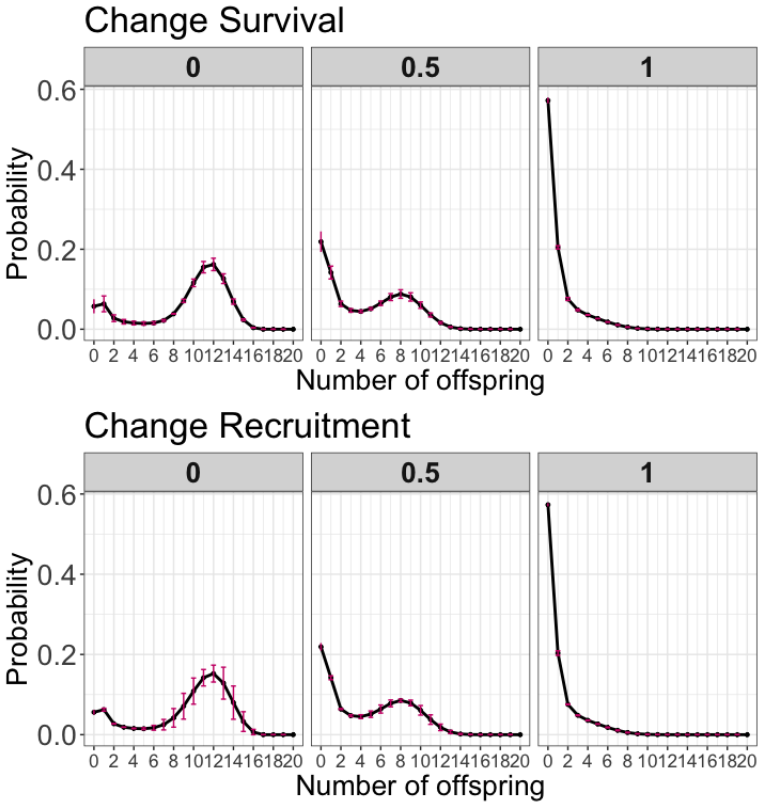

Figure 5: Plot for distribution of LRS. The top-three panels correspond to LRS distribution when only survival parameters are sampled from the covariance matrix and the rest of the parameters are fixed to their mean values. The bottom-three panels correspond to LRS distribution when only recruitment parameters are sampled and the rest of the parameters are fixed to their mean values. Each panel corresponds to a density scenario. Left most panel is for $N = 0$ case, followed by $N = K/2$, and $N = K$.

4 Discussion

We examine the interplay between life-history trade-offs and changes in density in Soay sheep. We use data from Kentie et al. (2020) to generate life-histories and found strong evidence for a trade-off between survival and growth during the juvenile stage at low density and between reproduction and juvenile survival at high density (Figure A4 and Figure 1 in Appendix). Thus, the nature of this trade-off is not static. The negative correlation and its explanatory power increase as population density increases. In addition, at carrying capacity (K) new trade-off arise between adult survival and juvenile survival. Thus, not all vital rates are equally impacted by changes in density, which gives rise to trade-offs. At low density, the demographic trade-off between growth and survival during the juvenile stage can be viewed as the main axis of life-history variation among individuals within population and aligns individuals along a slow-fast continuum similarly to what has been consistently reported across species (Stearns 1983; Oli 2004; Gaillard et al. 2016; Jiang et al. 2022; Van de Walle et al. 2023; Salguero-Gómez et al. 2016). However at high density, juvenile survival and reproduction structure life-history variation within the population.

Our findings are consistent with theory of life-history evolution (Stearns 1992) in that we find the evidence for trade-offs which prevent individuals from being proficient at both surviving and growing to large sizes. However, this markedly differs from previous analyses of intraspecific variation in life histories of vertebrates, which reported a lack of structuring axis of variation among individual life histories and no support for a slow-fast continuum (Van de Walle et al. 2023). This discrepancy might come from the absence of control for density dependence in previous studies. Alternatively, our simulated individual life histories might have included vital rate combinations that might have not been possible to observe in real individuals. Future work comparing potential (as investigated here) and realized (as analysed by Van de Walle et al. (2023)) variation in individual life history strategies should allow to explain this discrepancy.

Our results align with Kentie et al. (2020) as we find individuals with an average life history can not simultaneously maximise fitness for both high- and low-density environments. This is because demographic measures such as average survival, reproduction at SSD and distribution of lifetime reproductive success are highly constrained at high population densities (Figure 5). The level of variation and diversity at low population densities is not maintained at high population densities. Ozgul et al. (2009) found population density and maternal body size explain significant amounts of variation in temporal trends of mean body weight in Soay sheep. We find the contribution to reproduction at high population density comes from females of prime adult size ($\sim$ 25kg). However, at low densities reproductive contribution is from females of both small and large sizes. There is a concentration of individuals of prime size at high densities as shown in Figure A8 for stable stage distribution in Appendix. Increase in density may be a double whammy for females of small sizes since there is more competition and less individuals contribute to reproduction. However, individuals of large body size may allocate in producing few extremely fit offspring at high population densitie.

Our finding for probability of reproductive failure supports empirical evidence within Soay sheep population in the wild. At low density, juvenile mortality in Soay sheep is lower than the juvenile mortality at high density. Travis et al. (2023) provide a comprehensive review of density-dependent selection and how it may promote contrasting patterns of trait means at different population densities. Our research finds evidence for density-dependent effects on reproductive effort in natural populations, and aligns with r-K selection theory (Bassar et al. 2013). Our research predicts how density dependent influences strongly shape

the distribution of LRS and can lead to density-dependent selection since LRS is an important component of individual fitness. The decreasing complexity in life history variation at highest density does not support Lomnicki's prediction that individual differences should be more pronounced at high than at low density (Lomnicki 1978). On the contrary, our findings reveal that resource limitation constrains the size distribution of females in population, which thereby restrict individual variation in vital rates and demographic outcomes such as lifetime reproductive success.

There is empirical evidence for links between life-history trade-offs and density dependent selection from Drosophila cultures (Mueller and Ayala 1981; Mueller et al. 1991), insects (Gilbert and Manica 2010) and fisheries (Goodwin et al. 2006; Eikeset et al. 2016; Christie et al. 2018), among others. Mueller and Ayala (1981) studied populations of *Drosophila melanogaster* kept at low population densities (r-populations for about 200 generations) and then placed them in crowded cultures (K-populations). They found after 25 generations the K-populations showed higher growth rate and productivity at high densities (relative to the controls), but lower growth rate at low densities and experimentally confirmed fitness trade-offs can arise from density-dependent selection. A study (Sæther et al. 2016) on great tits *Parus major* showed females laying the largest clutch sizes at small population sizes experienced the greatest density-dependent reductions in fitness at large population sizes, thus providing empirical support for r- and K-selection. At small population sizes, phenotypes with large growth rates are favored, whereas phenotypes with high competitive skills are favored when populations are close to the carrying capacity K.

Our framework is general and can be applied to plant or animal species with individual-based life-history data such as, *Hypericum cumulicola* (Quintana-Ascencio and Morales-Hernández 1997), *Heliconia acuminata* (Brooks et al. 2019), *Poecilia reticulata* (Reznick et al. 2006; Bassar et al. 2016), and *Cervus elaphus* and (Gaillard et al. 2003). Our results are based on life-histories generated from the covariance matrix and don't correspond to data from real individuals. We also do not account for stochastic dynamics Lande et al. (2017) or climatic variation that has been found to affect population structure in Soay sheep (Ozgul et al. 2009). Further exploration of density effects can account for timing of reproduction and age-dependence of demographic parameters, especially senescence for which there has been a compelling evidence for many ungulate populations (Loison et al. 1999; Gaillard and Lemaıtre 2019).

5 Acknowledgements and funding sources

HJ, WZ, and ST would like to thank Stanford University for their funding. RK would like to thank University of Amsterdam and NIOZ as her funding sources. JMG and TC would like to thank University of Lyon and University of Oxford, respectively for their funding.

References

Agrawal, Anurag A, Jeffrey K Conner, and Sergio Rasmann (2010). "Tradeoffs and negative correlations in evolutionary ecology". *Evolution since Darwin: the first* 150, pp. 243–268.

Bassar, Ronald D, Andres Lopez-Sepulcre, David N Reznick, and Joseph Travis (2013). "Experimental evidence for density-dependent regulation and selection on Trinidadian guppy life histories". *The American Naturalist* 181.1, pp. 25–38.

Bassar, Ronald D et al. (2016). “The effects of asymmetric competition on the life history of Trinidadian guppies”. *Ecology Letters* 19.3, pp. 268–278.

Bell, Graham and Vassiliki Koufopanou (1991). “The architecture of the life cycle in small organisms”. *Philosophical Transactions of the Royal Society of London. Series B: Biological Sciences* 332.1262, pp. 81–89.

Brooks, Mollie E et al. (2019). “Statistical modeling of patterns in annual reproductive rates”. *Ecology* 100.7, e02706.

Cabana, Gilbert and Donald L Kramer (1991). “Random offspring mortality and variation in parental fitness”. *Evolution* 45.1, pp. 228–234.

Chesson, Peter (2003). “Quantifying and testing coexistence mechanisms arising from recruitment fluctuations”. *Theoretical population biology* 64.3, pp. 345–357.

Christie, Mark R, Gordon G McNickle, Rod A French, and Michael S Blouin (2018). “Life history variation is maintained by fitness trade-offs and negative frequency-dependent selection”. *Proceedings of the National Academy of Sciences* 115.17, pp. 4441–4446.

Clutton-Brock, TH et al. (1996). “Population fluctuations, reproductive costs and life-history tactics in female Soay sheep”. *Journal of Animal Ecology*, pp. 675–689.

Coulson, T et al. (2006). “Estimating individual contributions to population growth: evolutionary fitness in ecological time”. *Proceedings of the Royal Society B: Biological Sciences* 273.1586, pp. 547–555.

Coulson, Tim (2012). “Integral projections models, their construction and use in posing hypotheses in ecology”. *Oikos* 121.9, pp. 1337–1350.

Coulson, Tim, Steve Albon, Jill Pilkington, and Tim Clutton-Brock (1999). “Small-scale spatial dynamics in a fluctuating ungulate population”. *Journal of Animal Ecology*, pp. 658–671.

Coulson, Tim et al. (2001). “Age, sex, density, winter weather, and population crashes in Soay sheep”. *Science* 292.5521, pp. 1528–1531.

Czesak, Mary Ellen and Charles W Fox (2003). “Evolutionary ecology of egg size and number in a seed beetle: genetic trade-off differs between environments”. *Evolution* 57.5, pp. 1121–1132.

Descamps, S, J-M Gaillard, S Hamel, and NG Yoccoz (2016). “When relative allocation depends on total resource acquisition: implication for the analysis of trade-offs”. *Journal of evolutionary biology* 29.9, pp. 1860–1866.

Dobzhansky, Theodosius (1950). “Evolution in the tropics”. *American scientist* 38.2, pp. 209–221.

Eikeset, Anne Maria et al. (2016). “Roles of density-dependent growth and life history evolution in accounting for fisheries-induced trait changes”. *Proceedings of the National Academy of Sciences* 113.52, pp. 15030–15035.

Ellner, Stephen P, Dylan Z Childs, Mark Rees, et al. (2016). “Data-driven modelling of structured populations”. *A practical guide to the Integral Projection Model. Cham: Springer*.

Gaillard, Jean-Michel and Jean-François Lemaıtre (2019). “An aging phenotype in the wild”. *Science* 365.6459, pp. 1244–1245.

Gaillard, Jean-Michel et al. (2003). “Cohort effects and deer population dynamics”. *Ecoscience* 10.4, pp. 412–420.

Gaillard, Jean-Michel et al. (2016). “Life Histories, Axes of Variation in”. *The Encyclopedia of Evolutionary Biology*. Ed. by Richard Kliman. Elsevier, Academic Press, pp. 312–323. URL: https://hal-univ-lyon1.archives-ouvertes.fr/hal-02099457.

Gilbert, James DJ and Andrea Manica (2010). "Parental care trade-offs and life-history relationships in insects". *The American Naturalist* 176.2, pp. 212–226.

Goodwin, Nicholas B et al. (2006). "Life history correlates of density-dependent recruitment in marine fishes". *Canadian Journal of Fisheries and Aquatic Sciences* 63.3, pp. 494–509.

Grenfell, BT, OF Price, SD Albon, and TH Glutton-Brock (1992). "Overcompensation and population cycles in an ungulate". *Nature* 355.6363, pp. 823–826.

Hodgson, David J and Stuart Townley (2004). "Methodological insight: linking management changes to population dynamic responses: the transfer function of a projection matrix perturbation". *Journal of Applied Ecology* 41.6, pp. 1155–1161.

Horvitz, Carol, Douglas W Schemske, and Hal Caswell (1997). "The relative "importance" of life-history stages to population growth: prospective and retrospective analyses". *Structured-population models in marine, terrestrial, and freshwater systems*, pp. 247–271.

Jiang, Sha et al. (2022). "Reproductive dispersion and damping time scale with life-history speed". *Ecology Letters* 25.9, pp. 1999–2008.

Kentie, Rosemarie et al. (2020). "Life-history strategy varies with the strength of competition in a food-limited ungulate population". *Ecology Letters* 23.5, pp. 811–820.

Lande, Russell, Steinar Engen, and Bernt-Erik Sæther (2017). "Evolution of stochastic demography with life history tradeoffs in density-dependent age-structured populations". *Proceedings of the National Academy of Sciences* 114.44, pp. 11582–11590.

Loison, Anne et al. (1999). "Age-specific survival in five populations of ungulates: evidence of senescence". *Ecology* 80.8, pp. 2539–2554.

Lomnicki, Adam (1978). "Individual differences between animals and the natural regulation of their numbers". *The Journal of Animal Ecology*, pp. 461–475.

MacArthur, Robert H (1962). "Some generalized theorems of natural selection". *Proceedings of the National Academy of Sciences* 48.11, pp. 1893–1897.

Metcalf, C Jessica E (2016). "Invisible trade-offs: Van Noordwijk and de Jong and life-history evolution". *The American Naturalist* 187.4, pp. iii–v.

Mueller, Laurence D and Francisco J Ayala (1981). "Trade-off between r-selection and K-selection in Drosophila populations". *Proceedings of the National Academy of Sciences* 78.2, pp. 1303–1305.

Mueller, Laurence D, Pingzhong Guo, and Francisco J Ayala (1991). "Density-dependent natural selection and trade-offs in life history traits". *Science* 253.5018, pp. 433–435.

Norris, Ken and Matthew R Evans (2000). "Ecological immunology: life history trade-offs and immune defense in birds". *Behavioral Ecology* 11.1, pp. 19–26.

Oli, Madan K (2004). "The fast–slow continuum and mammalian life-history patterns: an empirical evaluation". *Basic and Applied Ecology* 5.5, pp. 449–463.

Ozgul, Arpat et al. (2009). "The dynamics of phenotypic change and the shrinking sheep of St. Kilda". *Science* 325.5939, pp. 464–467.

Pande, Jayant, Tak Fung, Ryan Chisholm, and Nadav M Shnerb (2020). "Mean growth rate when rare is not a reliable metric for persistence of species". *Ecology letters* 23.2, pp. 274–282.

Pande, Jayant, Yehonatan Tsubery, and Nadav M Shnerb (2022). "Quantifying invasibility". *Ecology Letters* 25.8, pp. 1783–1794.

Pianka, Eric R (1970). "On r-and K-selection". *The american naturalist* 104.940, pp. 592–597.

Quintana-Ascencio, Pedro F and Marina Morales-Hernández (1997). "Fire-mediated effects of shrubs, lichens and herbs on the demography of Hypericum cumulicola in patchy Florida scrub". *Oecologia* 112, pp. 263–271.
Reznick, D., M. Bryant, and D. Holmes (2006). "The Evolution of Senescence and Post-Reproductive Lifespan in Guppies (Poecilia reticulata)". *PLOS BIOLOGY* 4.1, p. 136.
Roff, D.A. (1992). *The Evolution of Life Histories: Theory and Analysis*. Chapman & Hall.
Roughgarden, Jonathan (1971). "Density-dependent natural selection". *Ecology* 52.3, pp. 453–468.
Sæther, Bernt-Erik, Marcel E Visser, Vidar Grøtan, and Steinar Engen (2016). "Evidence for r-and K-selection in a wild bird population: a reciprocal link between ecology and evolution". *Proceedings of the Royal Society B: Biological Sciences* 283.1829, p. 20152411.
Salguero-Gómez, Roberto et al. (2016). "Fast–slow continuum and reproductive strategies structure plant life-history variation worldwide". *Proceedings of the National Academy of Sciences* 113.1, pp. 230–235.
Simmonds, Emily G and Tim Coulson (2015). "Analysis of phenotypic change in relation to climatic drivers in a population of Soay sheep Ovis aries". *Oikos* 124.5, pp. 543–552.
Smith, Christopher C and Stephen D Fretwell (1974). "The optimal balance between size and number of offspring". *The American Naturalist* 108.962, pp. 499–506.
Stearns, Stephen C (1983). "The influence of size and phylogeny on patterns of covariation among life-history traits in the mammals". *Oikos*, pp. 173–187.
— (1989). "Trade-offs in life-history evolution". *Functional ecology* 3.3, pp. 259–268.
— (1992). *The Evolution of life histories*. Oxford: Oxford University Press.
Steiner, Ulrich K, Shripad Tuljapurkar, and Tim Coulson (2014). "Generation time, net reproductive rate, and growth in stage-age-structured populations". *The American Naturalist* 183.6, pp. 771–783.
Tatarenkov, Andrey, Christiane IM Healey, Gregory F Grether, and John C Avise (2008). "Pronounced reproductive skew in a natural population of green swordtails, Xiphophorus helleri". *Molecular ecology* 17.20, pp. 4522–4534.
Travis, Joseph et al. (2023). "Density-dependent selection". *Annual Review of Ecology, Evolution, and Systematics* 54, pp. 85–105.
Tuljapurkar, Shripad et al. (2020). "Skewed distributions of lifetime reproductive success: beyond mean and variance". *Ecology letters* 23.4, pp. 748–756.
— (2021). "Distributions of LRS in varying environments". *Ecology letters* 24.7, pp. 1328–1340.
Van de Walle, Joanie et al. (2023). "Individual life histories: neither slow nor fast, just diverse". *Proceedings of the Royal Society B* 290.2002, p. 20230511.
Van Noordwijk, Arie J and Gerdien De Jong (1986). "Acquisition and allocation of resources: their influence on variation in life history tactics". *The American Naturalist* 128.1, pp. 137–142.
Venable, D Lawrence (1992). "Size-number trade-offs and the variation of seed size with plant resource status". *The American Naturalist* 140.2, pp. 287–304.
Zera, Anthony J and Lawrence G Harshman (2001). "The physiology of life history trade-offs in animals". *Annual review of Ecology and Systematics* 32.1, pp. 95–126.

A Appendix A

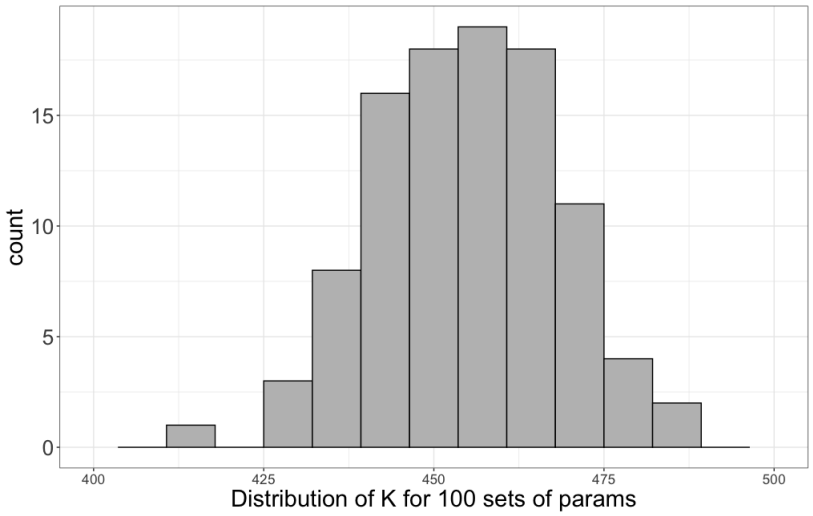

Figure A1: Equilibrium Distribution: mean 454

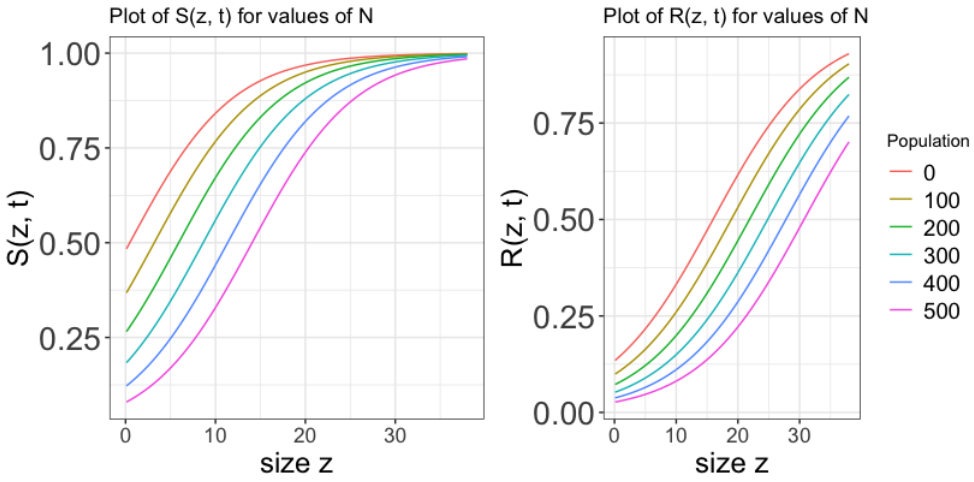

Figure A2: Plot of Survival and Recruitment functions for different values of Population, N.

Figure A3: Table 2: Table of PCA loadings for the Principal Components.

	PC1	PC2	PC3	PC4	N
Juv. Survival	-0.6879697	0.12862049	0.1212322	-0.7038872	0
Ad. Survival	-0.686233	-0.0630279	0.2061516	0.69470369	0
Reproduction	-0.2023425	-0.6648947	-0.7174507	-0.047297	0
Growth	0.1218173	-0.7330752	0.65426962	-0.1403301	0
Juv. Survival	0.68750662	-0.0194718	0.39635595	-0.6081591	K/2
Ad. Survival	0.68088722	0.20812351	-0.1056572	0.69420008	K/2
Reproduction	0.04627893	0.72806789	-0.585899	-0.3528424	K/2
Growth	-0.2481642	0.65285726	0.69889976	0.15404882	K/2
Juv. Survival	-0.6428758	0.01294431	-0.1599549	0.74897098	K
Ad. Survival	0.25436365	-0.7802743	-0.560259	0.11216476	K
Reproduction	0.61068116	-0.0551793	0.4797481	0.62758707	K
Growth	0.38610661	0.62286408	-0.6560229	0.18054366	K

Figure A4: Correlation Matrices for the three population densities. The top most panel corresponds to $N = 0$, followed by $N = K/2$, and $N = K$. The colors red, blue, and white correspond to negative, positive and no correlation.

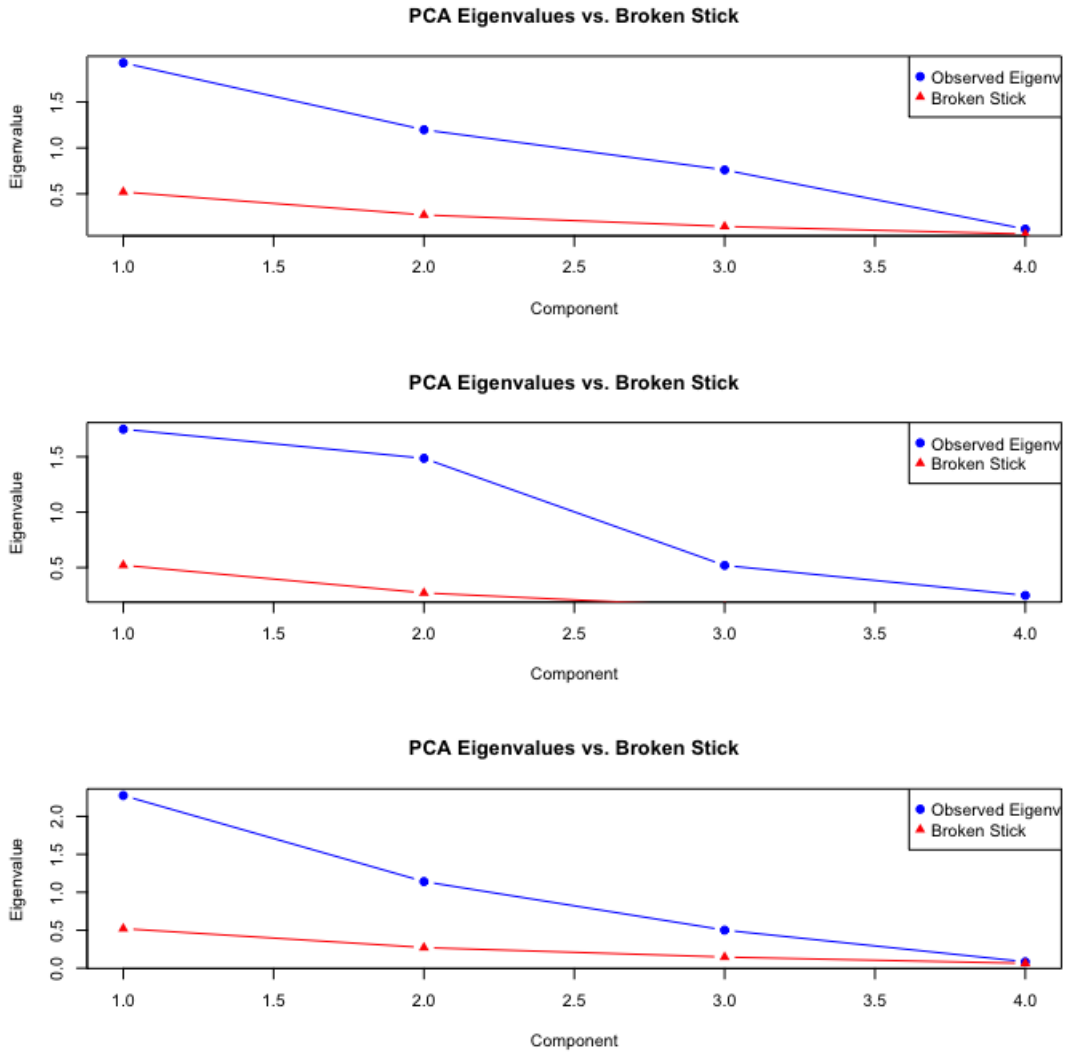

Figure A5: Eigenvalues from data and broken stick model. The top most panel corresponds to $N = 0$, followed by $N = K/2$, and $N = K$. Blue corresponds to observed eigenvalues from the data and red corresponds to eigenvalues from the broken stick model.

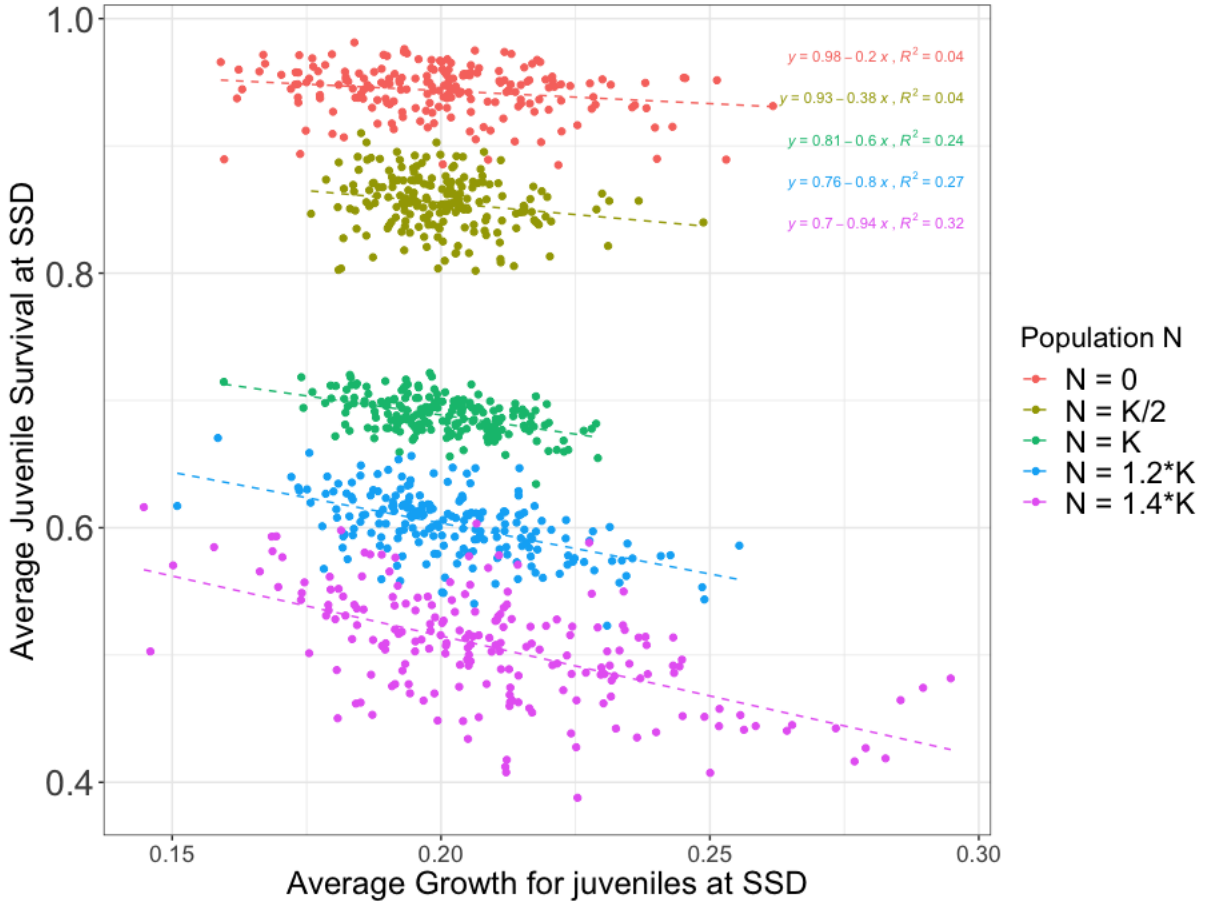

Figure A6: Plot for negative association between average growth increment for juveniles at SSD on the x-axis and average juvenile survival at SSD on the y-axis. The colors correspond to population density at $N = 0$, $N = K/2$, $N = K$, $N = (1.2)K$, and $N = (1.4)K$.

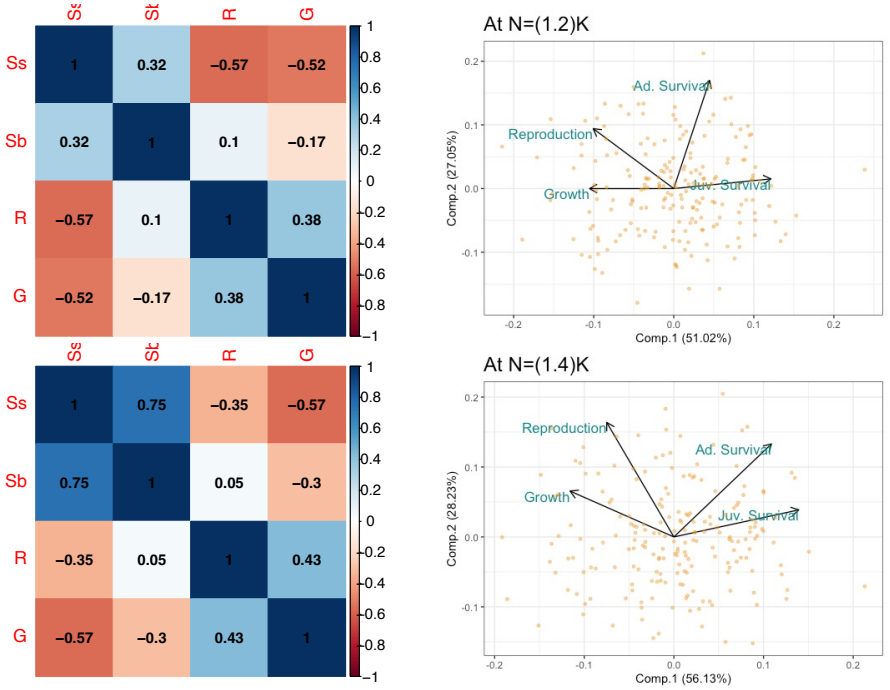

Figure A7: The top two panels show the correlation matrix and corresponding PCA at $N = 1.2K$. The bottom panels correspond to $N = 1.4K$. The colors red, blue, and white correspond to negative, positive and no correlation.

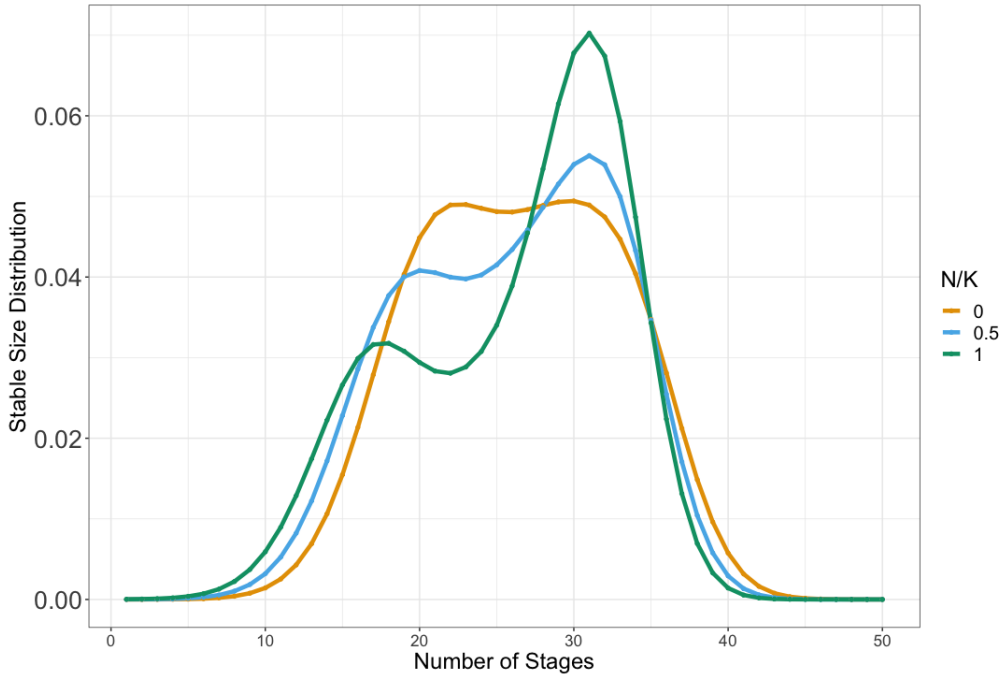

Figure A8: Stable Stage Distribution at different ratios of equilibrium population size. The legend $N/K = 0, 0.5,$ and 1 correspond to $N = 0$, $N = K/2$, and $N = K$.

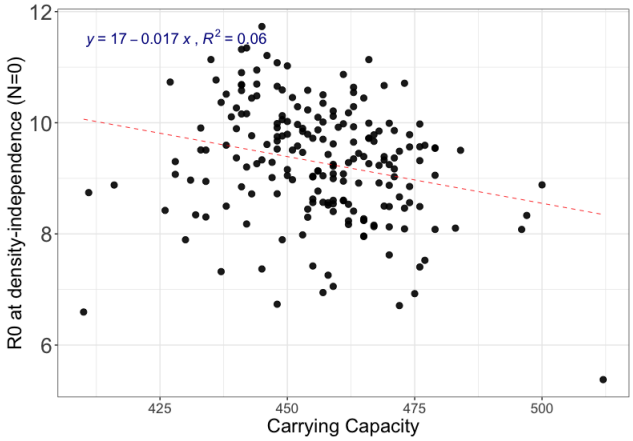

Figure A9: The plot shows negative correlation between carrying capacity, K on the x-axis and R_0 at $N = 0$ on the y-axis.

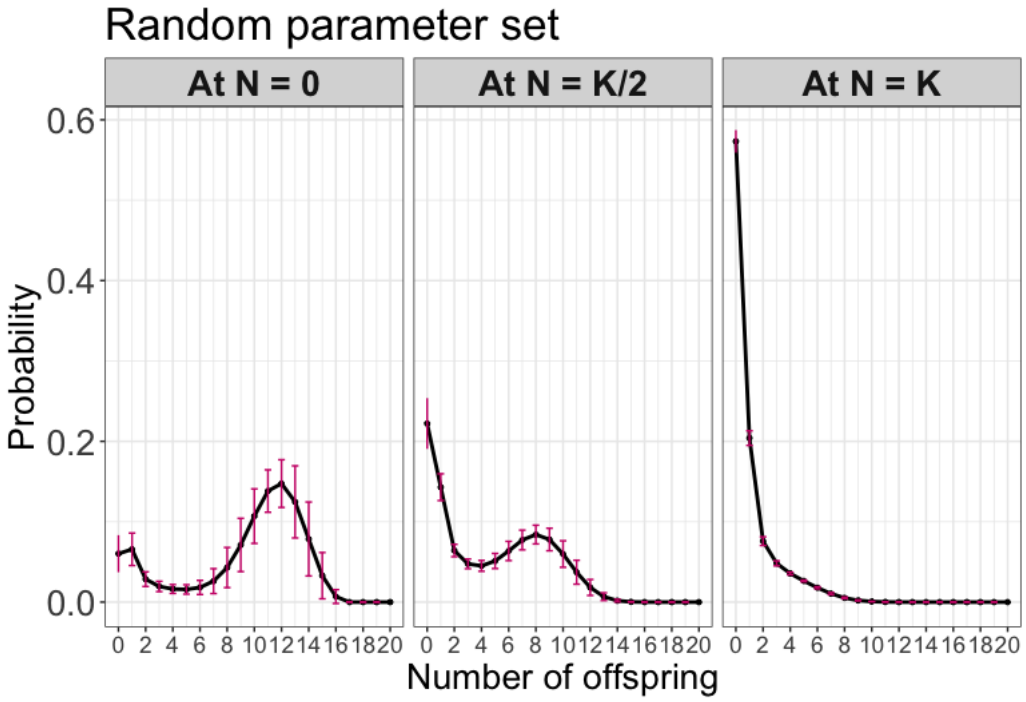

Figure A10: Distribution of LRS when all parameters are sampled from the covariance matrix at different population densities.

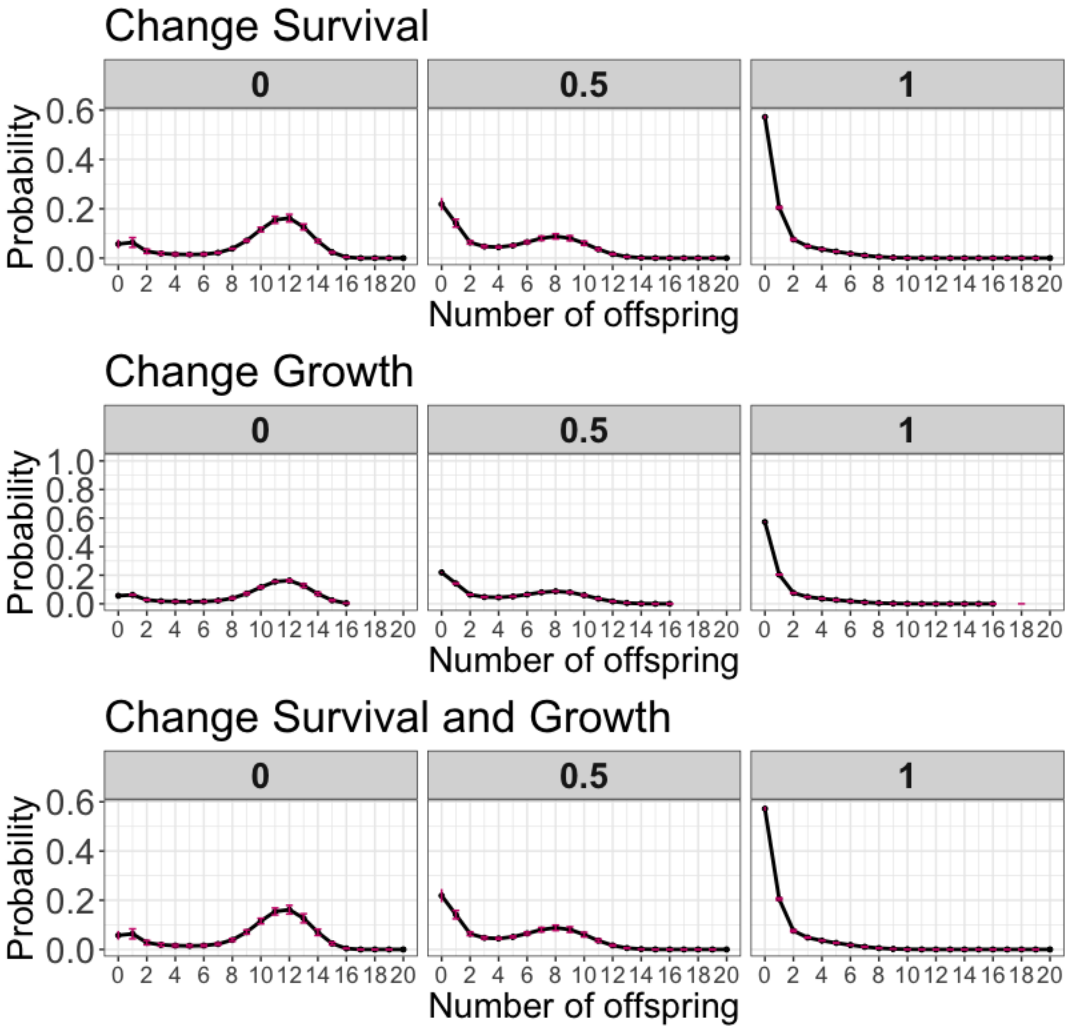

Figure A11: Distribution of LRS when survival and growth parameters are sampled from the covariance matrix at different population densities. The first and second panel correspond to varying survival and growth parameters. The third panel corresponds to varying both survival and growth parameters simultaneously.